

Optimization of modulation-doped $\text{Ga}_{1-x}\text{In}_x\text{As}/\text{InP}$ heterostructures towards extremely high mobilities

Hilde Hardtdegen, R. Meyer, M. Hollfelder, Th. Schäpers, J. Appenzeller, Hilde Løken-Larsen, Th. Klocke, Christel Dieker, B. Lengeler, and H. Lüth

Institut für Schicht- und Ionentechnik, Forschungszentrum Jülich, P.O. Box 1913, D-W-5170 Jülich, Germany

W. Jäger

Institut für Festkörperforschung, Forschungszentrum Jülich, P.O. Box 1913, D-W-5170 Jülich, Germany

(Received 8 July 1992; accepted for publication 19 January 1993)

This paper presents a study of the electrical and structural properties of inverted modulation-doped GaInAs/InP heterostructures grown by low-pressure metalorganic vapor phase epitaxy. First, the thickness of the GaInAs layer was optimized in lattice-matched samples to find the smallest thickness in which high Hall mobility is observed. Next, in a section closest to the InP the In content was varied. A steady increase of mobility with indium composition was observed. A maximum of 450 000 and 15 500 cm^2/Vs was obtained for a 10-nm-thick $\text{Ga}_{1-x}\text{In}_x\text{As}$ layer with $x=0.77$ at 6 and 300 K, respectively. Channels with higher indium content exceed the critical thickness and mobility drops off sharply. The decreasing mobility correlates with the formation of misfit dislocations at the interface indicating increasing scattering processes of the GaInAs layer.

I. INTRODUCTION

Epitaxially grown compound semiconductor films exhibiting high Hall mobilities have become increasingly important for application in fast devices. The $\text{Ga}_{1-x}\text{In}_x\text{As}/\text{InP}$ material system has particular advantages over other compound semiconductors: not only does it exhibit exceptionally high mobility at room temperature, it is also well suited for photon emission. This material system therefore allows fabrication of integrated circuits containing both high speed and photonic devices. An important requirement is to understand how to systematically obtain high Hall mobility. It has been demonstrated that increasing the indium content of the $\text{Ga}_{1-x}\text{In}_x\text{As}$ channel material in $\text{AlInAs}/\text{GaInAs}/\text{InP}$ MODFET (modulation-doped field-effect transistor) type structures leads to an improvement of the transconductance.¹ It also leads to extremely high Hall mobility in the channel which is of interest for the study of quantum and ballistical devices at liquid-He temperature.

Our aim in the present study was to reproducibly obtain the highest possible mobility in the $\text{Ga}_{1-x}\text{In}_x\text{As}/\text{InP}$ system and at the same time place the two-dimensional electron gas (2DEG) as near as possible to the sample surface. The inverted heterostructure under investigation consisted of a modulation-doped InP buffer layer and a lattice-matched GaInAs cap layer. We first determined the optimum thickness of the GaInAs layer in lattice-matched samples. Subsequently, in a 10-nm-thick part of this layer near the GaInAs/InP interface, which we will designate as "channel layer," the In content was varied. It will be shown, that an indium content of 0.77 in the channel layer leads to the highest 6 K mobility ever reproducibly obtained in this material system.

II. EXPERIMENTAL

The GaInAs/InP modulation-doped heterostructures were grown on $(001) \pm 0.5^\circ$ oriented substrates (Crismatec InPact) at 910 K in a horizontal low-pressure MOVPE reactor equipped with a vent run switching manifold using TMG, TMI, AsH_3 , PH_3 and the dopant gas H_2S in a hydrogen carrier. The total pressure was kept at 20 hPa and the gas velocity at 2.1 m/s to provide a rapid exchange of the gas phase when switching to the growth of a new layer. A growth interruption of 5 s was used at the InP/GaInAs interface. The switching sequence applied is described in Ref. 2. Two different TMI sources were employed so that the GaInAs channel and cap layers—both having different indium content—could be deposited with a growth interruption of only 3 s. The total gas flow in the vent and run lines were kept constant during the whole process (i.e., also during the switching sequences).

Since the composition of the $\text{Ga}_{1-x}\text{In}_x\text{As}$ layers cannot be determined on the modulation-doped structure itself, it was measured on 200-nm-thick layers deposited immediately after the modulation-doped structure using the same growth parameters by sputtered neutral mass spectrometry (SNMS), Rutherford backscattering spectrometry (RBS), and energy dispersive x ray (EDX). The EDX measurements were calibrated with two samples of known indium content: a lattice-matched sample (lattice match determined by x-ray diffraction) and a 200-nm-thick GaAs layer (0% indium content) on an InP substrate. SNMS measurements were calibrated with a lattice-matched sample.

Electrical characterization of the modulation-doped heterostructures was carried out using the Hall effect. These investigations were performed employing the van der Pauw geometry in the temperature range from 5 to 300

K and at a magnetic field strength of 0.4 T. Indium pellets alloyed at 620 K were used for ohmic contacts. In addition, Shubnikov-de Haas oscillations and the quantum Hall effect were investigated in a selection of samples. In order to perform these measurements Hall bars fabricated by optical lithography were prepared. The mesa was defined using 1 n K₂Cr₂O₇, H₃PO₄, HBr (1:2:2).³ Ni/AuGe/Ni (25 nm/90 nm/5 nm) alloyed at a temperature of 670 K was used for ohmic contacts. All measurements were carried out in the dark. The low-frequency lock-in technique was used. The measurement current never exceeded 2 μ A.

The structure of the multilayers was studied by transmission electron microscopy (TEM). The characterizations were performed with a JEOL 4000 FX electron microscope at 400 kV on (001) plan-view and (110) cross-section specimens prepared by iodine-assisted Ar⁺ milling.

III. RESULTS

A. Composition

The gallium to indium ratio in the crystalline layer was found to be directly proportional to the ratio of the corresponding partial pressures in the gas phase [$0.703 \times p_{\text{TMI}}/p_{\text{TMG}} = x_{\text{In}}/(1-x_{\text{In}})$] within the margin of error of all analytical methods used and with $R^2=0.965$. The proportionality factor c was obtained from a lattice-matched sample, this condition being established with the help of x-ray diffraction. The margin of error in the composition of the SNMS, EDX, and RBS measurements was determined to be 1%, 1%, and 5%, respectively.

B. Electrical characteristics

Earlier investigations of modulation-doped GaInAs/InP structures⁴ showed that layer parameters like dopant concentration and spacer thickness strongly influence electron mobility, sheet carrier concentration, and subband population in the 2DEG. Our aim was to reproducibly prepare structures with the highest possible mobility at low temperatures. To this end a 20 nm InP spacer thickness was chosen between dopant spike and channel. Earlier studies have shown that this thickness presents a good compromise between the requirements for sufficient separation of dopant ions from the 2DEG and efficient transfer of electrons to the channel.⁴ In this earlier work the highest mobilities were obtained when one subband was completely filled. This was the case for a dopant concentration of $4.2 \times 10^{17} \text{ cm}^{-3}$ in a 10-nm-thick dopant spike.

We first studied samples with GaInAs channels lattice matched to InP using the layer parameters mentioned above. The thickness of the GaInAs layer was varied between 0.05 and 1.2 μm to establish the minimum thickness for which high mobility is still obtained in the 2DEG. There are several reasons for such an approach: the transconductance of the MODFET using this system increases with decreasing GaInAs thickness; it becomes easier to contact the 2DEG region; when the cap layer is thin enough a superconductor may be able to contact the 2DEG (proximity effect) without etching all together.

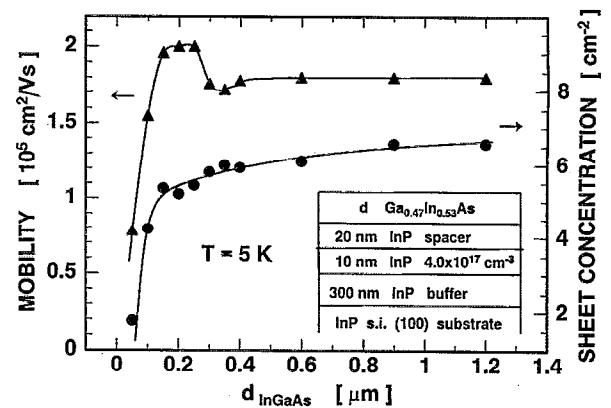


FIG. 1. Dependence of Hall mobility and sheet carrier concentration at 5 K on Ga_{0.47}In_{0.53}As layer thickness. At a layer thickness below 150 nm the mobility drops off sharply.

Figure 1 shows the dependence of Hall mobility at 5 K on the thickness of the GaInAs layer. When decreasing the thickness the mobility remains constant until 300 nm. A slight increase from 180 000 to 200 000 cm²/V s is then observed. Below 150 nm the mobility curve drops off abruptly. 150 nm is apparently the minimum GaInAs thickness with which high mobility values are obtained.

The dependence of sheet carrier concentration on GaInAs layer thickness is also presented in Fig. 1. Starting at low thicknesses the sheet carrier concentration first increases strongly with layer thickness. Above 400 nm the sheet carrier concentration increases more slowly and appears to saturate. To explain this dependence we should recall that the surface of the GaInAs contains a depleted zone. For lattice-matched GaInAs with a background carrier concentration of $2 \times 10^{15} \text{ cm}^{-3}$, this extends over nearly 400 nm. If GaInAs layers are thinner than this value the GaInAs layer is completely depleted. In this case electrons that otherwise would contribute to the 2DEG are localized in surface states. On the other hand, when the GaInAs layer thickness exceeds 400 nm carriers resulting from background doping will also contribute to the conductance.

The dependence of the 5 K Hall mobility on the sheet carrier concentration is presented in Fig. 2. Up to a concentration of $5.4 \times 10^{11} \text{ cm}^{-2}$ the mobility increases. Above this concentration it shows a distinct drop but increases again for larger concentrations. We propose that at a concentration just above $5.4 \times 10^{11} \text{ cm}^{-2}$ a second subband is populated and gradually filled. Intersubband scattering has a large effect on the mobility when the second subband starts to be populated^{5,6}: there is a sudden drop in mobility. The mobility increases again the more the 2DEG is screened from the impurity ions by increasing electron concentration. Shubnikov-de Haas and quantum Hall-effect measurements were carried out on two of these samples to check on this assumption. One of the samples exhibited a Hall mobility at the peak in the mobility curve, the other was selected from the higher concentration range. In the first case only one set of oscillations was observed [Fig. 3(a)], no conducting bypass channel was found. In the

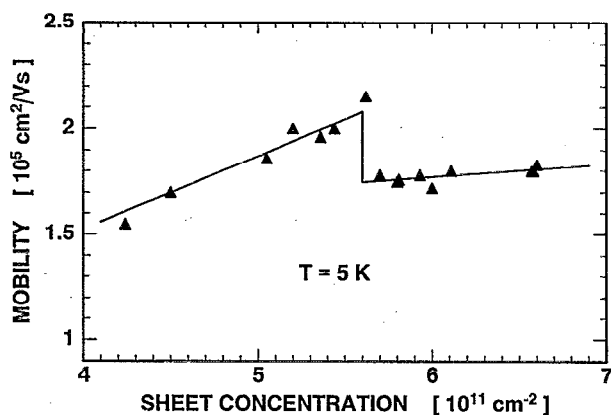


FIG. 2. Dependence of Hall mobility on sheet carrier concentration at 5 K in $\text{Ga}_{0.47}\text{In}_{0.53}\text{As}$. A distinct drop in mobility is observed for a sheet carrier concentration just above $5.4 \times 10^{11} \text{ cm}^{-2}$.

other case two sets of oscillations were found [Fig. 3(b)]. They could be assigned to two subbands. These findings thus confirm our assumption that intersubband scattering reduces 5 K Hall mobility at sheet carrier concentrations above $5.4 \times 10^{11} \text{ cm}^{-2}$.

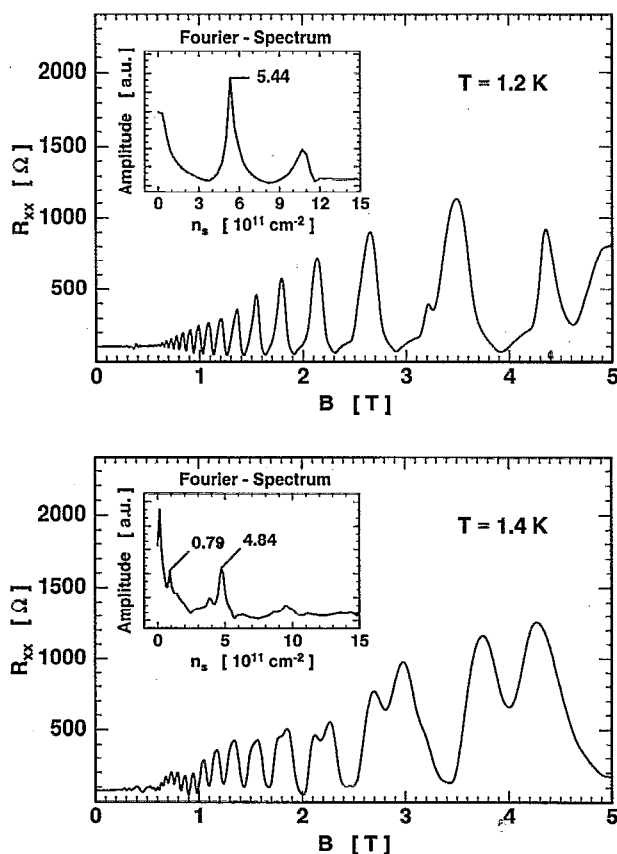


FIG. 3. Shubnikov-de Haas (R_{xx}) in $\text{Ga}_{0.47}\text{In}_{0.53}\text{As}$ for a modulation-doped structure (a) with one subband occupied, i.e., sheet carrier concentration below $5.4 \times 10^{11} \text{ cm}^{-2}$; (b) two subbands occupied: the first with a density $n_s = 4.84 \times 10^{11} \text{ cm}^{-2}$, the second with $0.79 \times 10^{11} \text{ cm}^{-2}$.

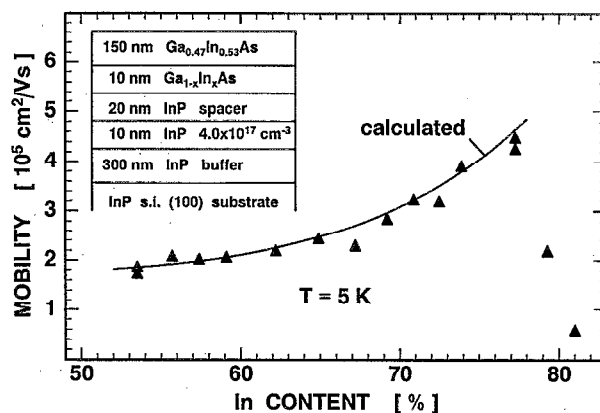


FIG. 4. Dependence of Hall mobility at 5 K on In content in $\text{Ga}_{1-x}\text{In}_x\text{As}/\text{InP}$ heterostructures; points: measured values; line: calculated values based on power law dependence on carrier concentration $\mu \sim n_s^{0.6}$.

On the basis of these findings an optimum thickness of 150 nm was established. At this thickness the sheet carrier concentration reaches the optimum value of $5.4 \times 10^{11} \text{ cm}^{-2}$. For such a structure mobilities of 190 000 and 10 400 cm^2/Vs were obtained at 5 and 300 K, respectively.

After having obtained the optimum cap layer thickness for lattice-matched GaInAs samples, we introduced a 10-nm-thick channel layer into our modulation-doped structure in which we successively increased the indium content in order to achieve the highest possible mobility. Since alloy scattering shows a maximum at $x=0.5$, i.e., in the lattice-matched case, an increase in In content reduces alloy scattering. Low-temperature mobility, which is restricted by alloy scattering, increases. At the same time the effective electron mass decreases which is an important factor for room- and low-temperature mobility. In $\text{Ga}_{1-x}\text{In}_x\text{As}$ the highest effective mass is observed for $x=0.0$ and the lowest for $x=1.0$. We therefore explored the dependence of the Hall mobility on the indium content in the channel.

As shown in Fig. 4 the low-temperature Hall mobility steadily increases with indium content in the channel and reaches a maximum of 450 000 cm^2/Vs for $x=0.77$. Above this x value the mobility drops off abruptly. Increasing the In content by only 1% leads to a drop in mobility by a factor of 2. As shown in the next section, at this composition the 10 nm channel layer exceeds the critical thickness and relaxation of the strain in the layer by plastic flow sets in.

We also observed a slight linear increase in sheet carrier concentration with indium content. This can be explained from the more efficient transfer of electrons into the quantum well as the band discontinuity increases. We were interested in how the mobility of strained samples (μ) relates to the mobility of lattice-matched ones (μ_{lm}). The solid line in Fig. 4 results from a mobility calculation taking into account the indium content x and x_{lm} , the effective electron masses m^* and m_{lm}^* and the net carrier concentration in the conducting channel n and n_{lm} of the

strained and lattice-matched (lm) samples, respectively. The two limiting scattering contributions are the alloy scattering $\mu_{\text{al}} \sim m^{*-5/2}/x(x-1)$ and ionized impurity scattering $\mu_{\text{imp}} \sim m^{*-1/2}$. Due to the dominance of the alloy scattering we assumed a square dependence of m^* on the mobility.⁷ The mobility for the strained samples is related to the mobility for the lattice matched samples as follows:

$$\mu = \mu_{\text{lm}} \frac{x_{\text{lm}}(1-x_{\text{lm}})}{x(1-x)} \left(\frac{m_{\text{lm}}^*}{m^*} \right)^2 \left(\frac{n}{n_{\text{lm}}} \right)^{0.6}$$

The values for the effective masses were extrapolated from theoretical values.^{8,9}

The room-temperature mobility also increases, namely, from 10 400 cm²/V s for the lattice-matched channel to 15 500 cm²/V s for an indium content of $x=0.77$. The decrease in electron mass is responsible for this effect. Studies are presently in progress to show the effect of the high mobility gate structure on the characteristics of MODFETs.

At last we varied the channel layer thickness between 9 and 11 nm for In concentrations near the maximum of the mobility curve—namely, 74%, 76%, and 78%—to check if the 10 nm chosen for the HEMT structure are a reasonable thickness. In all three cases the highest mobility is observed for the 10-nm-thick channel. The decrease in mobility for larger channel widths can be attributed to formation of misfit dislocations due to strain relaxation. Even in the sample with 74% In content where the critical layer thickness was not exceeded (as seen by TEM), the increased channel layer thickness did not lead to higher mobility. For smaller channel widths the electron wave function extends into the lattice-matched cap layer leading to an increasing average electron mass and alloy scattering and therefore decreasing mobility. Obviously, the chosen channel thickness is a good compromise.

C. Structural characteristics

A series of five samples with indium contents x between 0.53 and 0.80 in the channel were studied to be able to correlate electrical data to structural properties of the same sample. Figure 5 shows a TEM micrograph of the sample with the highest low-temperature mobility (In content 77%) in cross section. It is an example of the excellent homogeneity of the channel layer thickness these structures show. The thickness is in good agreement with the nominal thickness (10 nm). Both interfaces are abrupt and planar.

At an In content lower than 77% misfit dislocations were not observed indicating dislocation spacings $> 100 \mu\text{m}$. A few large precipitates were found in the structure with diameters of $\approx 250 \text{ nm}$. They were not only observed in the channel but also in the buffer layer. Their origin could not be determined. Possibly they originate from cleavage of the wafer before epitaxy (we only employed a quarter of a wafer per growth run).

At higher In content ($x=0.78$, $x=0.80$) networks of misfit dislocations at the channel interface were observed

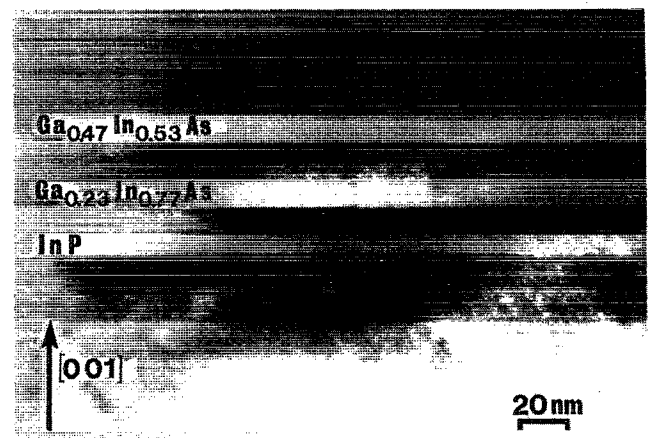


FIG. 5. Strained $\text{Ga}_{0.47}\text{In}_{0.53}\text{As}/\text{Ga}_{0.23}\text{In}_{0.77}\text{As}/\text{InP}$ (001) heterostructure. TEM bright field micrograph of cross-section specimen, $\langle 110 \rangle$ projection with electron beam parallel to (001) interfaces showing the homogeneity of the channel layer thickness.

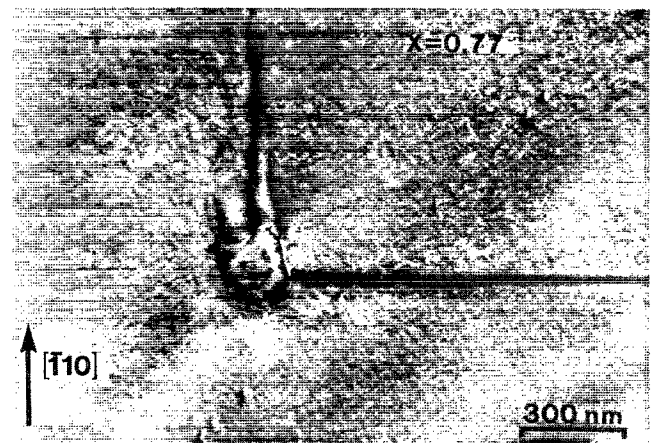
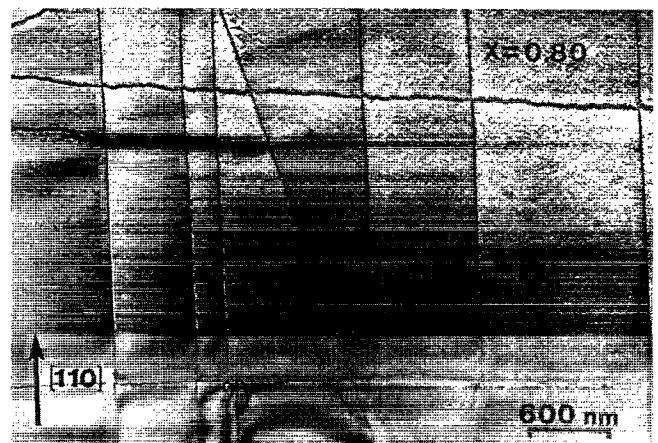


FIG. 6. (a) Network of misfit dislocations at $\text{Ga}_{1-x}\text{In}_x\text{As}$ interface for $x=0.80$ leading to a drop in mobility. TEM bright field micrograph of plan-view specimen near (001) projection; (b) TEM bright field micrograph of a sample with a $\text{Ga}_{0.23}\text{In}_{0.77}\text{As}$ channel, cross section in $\langle 110 \rangle$ projection with electron beam parallel to (001) interfaces showing an interface precipitate with dislocation segments. These segments do not influence mobility.

[Fig. 6(a)]. Most of the dislocation lines are parallel to $\langle 110 \rangle$ directions which is consistent with the conventional glide of misfit dislocations on 111 resulting in 60° dislocations with $b=1/2 \langle 101 \rangle$. Average dislocation densities are $1.5 \times 10^4 \text{ cm}^{-1}$. Precipitates are also observed and are nearly always connected to dislocations belonging to the network. A few of the precipitates are connected to threading dislocations also observed in both samples. The decrease in mobility for In concentrations above 77% can clearly be attributed to the formation of dislocation networks indicating increasing scattering processes as the strain relaxes.

At $x=77\%$ precipitates and dislocation segments threading to the surface are also present. Most of the precipitates are connected to dislocations [Fig. 6(b)]. Planar networks of misfit dislocations are absent. In some areas, however, indications for the onset of network formation exist. In conclusion as long as no dislocation network is formed, extremely high mobilities can be obtained.

IV. CONCLUSIONS

In this study we have demonstrated the possibility to reproducibly grow $\text{Ga}_{1-x}\text{In}_x\text{As}/\text{InP}$ modulation-doped heterostructures by LP-MOVPE with extremely high mobility. The mobility is influenced by the thickness of the GaInAs layer. It was also shown that the composition of the part of this layer adjacent to the InP spacer is a further determining factor for the value of the mobility at liquid helium and room temperature. When exceeding a certain value of the In concentration the films relax and generation of a misfit dislocation network causes the mobility to drop off sharply. Compared to the use of an optimized GaInAs

layer only introduction of a 10-nm-thick layer with the optimum In content (77%) gives rise to an increase of the mobility from 200 000 to 450 000 $\text{cm}^2/\text{V s}$ at liquid-He temperature and from 10 400 to 15 500 $\text{cm}^2/\text{V s}$ at room temperature.

ACKNOWLEDGMENTS

The authors would like to thank P. Balk (Delft Institute of Microelectronics and Submicron Technology, TU Delft) for fruitful discussions, K. Schmidt (Institut für Schicht- und Ionentechnik, Forschungszentrum Jülich) for RBS analysis, U. Breuer (Institut für Halbleitertechnik, RWTH Aachen) for SNMS analysis, R. Mitdank (Institut für Ionen- und Elektronenphysik, FB-Physik der Humboldt-Universität Berlin) for EDX measurements, and K. Wirtz for technical assistance.

- ¹U. K. Mishra, A. S. Brown, M. J. Delaney, P. T. Greiling, and C. F. Krumm, *IEEE Trans. Microwave Theory Technol.* **37**, 1279 (1989).
- ²D. Grützmacher, J. Hergeth, F. Reinhardt, K. Wolter, and P. Balk, *J. Electron. Mater.* **19**, 471 (1990).
- ³S. Adachi, *J. Electrochem. Soc.* **129**, 609 (1980).
- ⁴D. Grützmacher, R. Meyer, M. Zachau, P. Helgesen, A. Zrenner, K. Wolter, H. Jürgensen, F. Koch, and P. Balk, *J. Cryst. Growth* **93**, 382 (1988).
- ⁵H. L. Störmer, A. C. Gossard, and W. Wiegmann, *Solid State Commun.* **41**, 707 (1982).
- ⁶W. Walukiewicz, H. E. Ruda, J. Lagowski, and H. C. Gatos, *Phys. Rev. B* **30**, 4571 (1984).
- ⁷A. Chin and T. Y. Chang, *J. Vac. Sci. Technol. B* **8**, 364 (1990).
- ⁸M. Jaffe and J. Singh, *J. Appl. Phys.* **65**, 329 (1989).
- ⁹Y. Foulon, C. Priester, G. Allan, and M. Lannoo, in *Proceedings of the 20th International Conference on the Physics of Semiconductors*, Thessaloniki, Greece, 1990, edited by E. M. Anastassakis and J. D. Joannopoulos (World Scientific, Singapore, 1990), Vol. 2, p. 977.